Journal of Materials Chemistry A

Accepted Manuscript

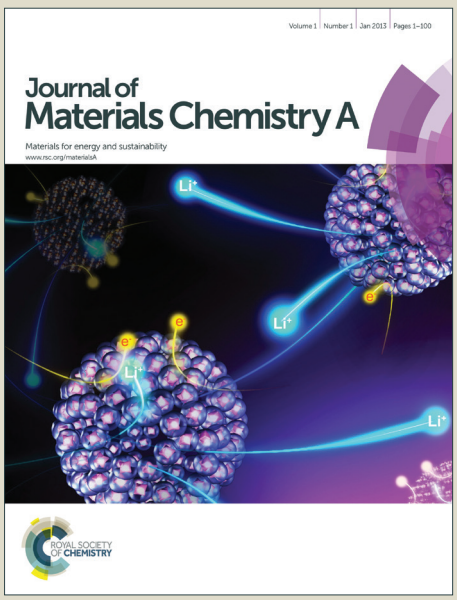

ROYAL SOCIETY OF CHEMISTRY

www.rsc.org/materialsA

Journal Name

RSCPublishing

ARTICLE

Fabrication of Titanium Phosphate@Graphene Oxide Nanocomposite and its Super Performance on Eu^{3+} Recycling

Cite this: DOI: 10.1039/x0xx00000x

Received 00th January 2012,
Accepted 00th January 2012

DOI: 10.1039/x0xx00000x

www.rsc.org/

Chaoran Li,[a] Yang Huang,[a] and Zhang Lin[a]*

Abstract: Despite its great potential as adsorbent, graphene oxide (GO) is still not widely used mainly due to the difficulties in redispersing after drying. In order to break the strong forces between GO layers and improve the adsorption ability, a titanium phosphate (TiP) modified GO composite was fabricated in this work. Hierarchically structured GO@TiP composites (GTiP) were synthesized via a mild in-situ chemical precipitation method. The products were thoroughly characterized by various methods such as SEM, TEM, XRD, XPS and BET. This new material was then applied as an adsorbent for Eu^{3+} in water. GTiP exhibited excellent adsorption characteristics for europium ions. It took shorter than 1.5 min to reach half-equilibrium, while its adsorption capacity can be as high as 64.33 mg g^{-1}. GTiP also shows great adsorption ability both in a wide range of pH and salinity. The superb adsorption capability of GTiP may have derived from both materials in that GO increased the specific surface area and adsorption capacity, while TiP enhanced hydrophilicity and mechanical properties of GTiP.

Introduction

With the rapid development of the nuclear industry, a large number of nuclear wastes are produced in the form of radioactive wastewater.[1,2] As an important goal in radioactive waste treatment, efficient immobilization of the radioactive actinides in the wastewater attracts intense research interest. Since europium (Eu) and actinides radionuclides are chemical homologues, study of Eu adsorption behavior on the solid-liquid interface between the adsorbent and adsorbate can help predict the effectiveness of adsorbents for radionuclides without the risks of radioactive exposure.[3,4] In fact, the study of Eu extraction can provide not only theoretical basis for radionuclide recycling, but also real economic benefits. With only a content of 0.000106% in earth, Eu is one of the scarcest and most expensive rare earth elements (REEs). On the other hand, as an important red phosphor activator, Eu is widely used in some of best phosphors for its outstanding luminous efficiency and the coating stability.[5] The conflict between the increasing demand in lighting industry and the limited amount of Eu draws forth the need for efficient recovery of Eu. In the past years, many adsorbents have been widely studied to extract Eu^{3+} from water.[4,6-10] However, the fatal flaw of low adsorption capacity (<10 mg/g) limited their practical application in the removal of radionuclides from large volumes of aqueous solutions.[11] Therefore, there is an urgent need for developing an adsorbent material with high adsorption capacity and efficiency, as well as the tolerance in a wide range of pH and salinity, which is also environmentally friendly, easily recyclable and renewable.

Graphene oxide (GO), which possesses a large specific surface area and rich carboxyl and hydroxyl groups, performs well in immobilizing various metal ions, such as Zn, Cu, Pb, Cd and Co.[12-14] Its adsorption capacity of Eu can reach as high as 175.44 mg/g.[11] However, there are some drawbacks of GO when used in large-scale wastewater treatment. First, the biggest obstacle in using GO for practical water treatment is its high cost. How to reduce the cost without affecting the adsorption efficacy is a realistic problem facing GO's further application. Second, GO reunites after drying, which reduces not only the specific surface area, but also its hydrophilicity, thus affecting the adsorption efficacy. Therefore, an ultrasonic pre-processing step is usually adopted. However, this step is impractical to perform in a large-scale wastewater treatment process. Third, the dispersed GO nanosheets after ultrasonic processing may stack and congest in the process of passing through a column which is a commonly used in practical wastewater treatment. As a result, the column efficiency would be reduced and solid-liquid separation would be difficult to achieve after the adsorption. To address these problems, a composited GO with another potential Eu adsorbent material is presented in this work. It is designed to lower the cost by reducing the consumption of GO and prevent the reunion by the composite materials evenly distributed on the surface of GO. We can also control the morphology of the composite to be self-supported which is kinetically favoured for maintaining the flow velocity in the extraction process while avoiding aggregation and clogging problems that nanomaterials frequently encounter.

It is known that phosphate ion (PO_4^{3-}) can combine with REEs firmly. It can therefore be speculated that a GO-PO_4^{3-} composite system might hold great potential for recycling Eu. An appropriate metal ion may be needed as a bridge to link free phosphate ion to the surface of GO. Tetravalent metals such as titanium, zirconium, etc. seem to be a good candidate. Titanium phosphate (TiP) is a kind of insoluble salt with many excellent properties comparing with organic polymers[15,16], metal hydroxide[17] and clay minerals.[18] Its high ion selectivity makes it possible to adsorb REEs from solutions containing high concentrations of Na^+ and K^+. Its high acid tolerance allows direct extraction of Eu from acidic solutions. TiP also has high chemical and thermal stability, ensuring the composite material possesses superb tolerance to complex composition of wastewater. Therefore, TiP modified GO is expected to be an ideal material with great potential in the recycling of Eu.

In this work, hierarchically structured GO@TiP nanocomposites

(GTiP) were synthesized by in-situ precipitation, followed by characterization using a variety of instrumental techniques. With the focus of evaluating its extraction efficacy of Eu ions from aqueous systems, adsorption isotherms of GTiP for Eu were generated and kinetics studied. The effects of solution pH and ionic strength were also investigated. Finally, the regeneration and reusability of GTiPs were examined.

Experimental section

Materials

All chemicals were used without further purification, and all solutions were prepared using deionized (DI) water. Titanium sulfate [$Ti(SO_4)_2$, CP], phosphoric acid (H_3PO_4, AR), sulfuric acid (H_2SO_4, AR), hydrochloric acid (HCl, AR), hydrogen peroxide (H_2O_2, AR), potassium permanganate ($KMnO_4$, AR), sodium chloride (NaCl, AR) and sodium nitrate ($NaNO_3$, AR) were obtained from Sinopharm Chemical Reagent Co., Ltd. of China. Graphite (SP) and europium chloride (AR) were purchased from Alfa Aesar and Aladdin Reagent (Shanghai) Co., Ltd., respectively.

Preparation of TiP

TiP was prepared by the precipitation method at a controlled temperature of 338 K. The same volume of 0.6 M H_3PO_4 was added dropwise to a 0.3 M $Ti(SO_4)_2$ solution at a stirring speed of 3000 rpm. After aging for 2 h, the suspension was centrifuged at 8000 rpm for 2 min and washed with distilled water three times. The precipitate was collected and dried for the X-ray powder diffraction (XRD) analysis, scanning electron microscope (SEM) study, and Brunauer-Emmett-Teller (BET) measurement.

Preparation of GO

GO was prepared using the modified Hummers' method.[19] Briefly, graphite powder was mixed with $NaNO_3$ and H_2SO_4. The reaction was done in an ice bath for 30 min. After that, the mixture was further oxidized by adding $KMnO_4$. The temperature was then raised and maintained at 308 K for 24 h. An appropriate amount of water was added and the temperature increased to 363 K with continuous stirring. The solution was further diluted and H_2O_2 was added to the solution to terminate the reaction. The product was centrifuged at 8000 rpm for 2 minutes and washed with 1.0 M HCl. Subsequent rounds of washing with water were done to bring the pH of the final product to neutral. The residue was finally washed with methanol and dried in a vacuum oven.

Preparation of GTiP nanocomposite

The GTiP nanocomposite was prepared by an in-situ precipitation process. The GO solution was prepared by dispersing 20 mg of GO powder in 20 mL of DI water followed by sonication for 30 min. The GO solution was mixed with $Ti(SO_4)_2$ solutions of different volumes at 338 K. With continuous stirring, appropriate amount of H_3PO_4 was added dropwise. After aging for 2 h, the suspension was centrifuged at 8000 rpm for 2 min and washed with distilled water three times. The precipitate was collected and dried.

Adsorption experiments

A simulated 200 mg L^{-1} Eu^{3+} solution (2 L) was prepared as the stock solution. Extraction of Eu^{3+} was performed without any pre-treatment with an adsorbent dosage of 1 mg mL^{-1}. Adsorption experiments were performed at room temperature. The mixtures of absorbent and Eu^{3+} solutions were filtered through polyether sulfone (PES) membranes (0.26 μm pore size). Eu^{3+} concentrations in the filtrates were analysed using inductively coupled plasma atomic emission spectrometry (ICP-AES).

Adsorpion kinetics. The mixture of absorbent and Eu^{3+} solution was stirred for 2 h until the saturated adsorption state was reached. During the process, the supernatant was sampled at a series of intervals.

Adsorption isotherms. To the Eu^{3+} solution were added GTiP samples of different initial concentrations ranging from 5 mg L^{-1} to 200 mg L^{-1}. Adsorption continued for 4 h with continuous stirring, which was found to be sufficient for the mixture to reach equilibrium. After equilibrium, the residual concentration was measured and the maximum adsorption capacity was calculated.

Effect of pH. The adsorption capacities of the absorbents were tested at different pHs. The pH of the Eu^{3+} solution was adjusted to 1.7, 3.7, 5.5 and 7.3 with 1 M NaOH or 1 M HCl. A pH meter was used for pH measurement.

Effect of ionic strength. Na^+ at concentration levels of 1, 10, 100, and 1000 mM was chosen to evaluate for the effect of competitive cation binding. The highest Na^+ concentration was about 1500 times higher than that of Eu^{3+}.

Recycling of adsorbent. The composites were added to 100 mL 100 mg L^{-1} Eu^{3+} solution at 1 mg mL^{-1} and equilibrated for 2 h. For regeneration, the composites were immersed in 10 mL of a 1 M HCl solution for 1 h, followed by DI water rinsing to neutral pH. Regenerated nanocomposites were used for adsorption in the succeeding cycles.

Characterization

The phases of the samples were identified by the XRD patterns obtained on a PANalytical X'Pert PRO diffractometer with Cu Kα radiation (40 kV, 40 mA) in the continuous scanning mode. The 2θ scanning range was from 5° to 85° in steps of 0.017° with a collection time of 20 s per step. The morphology and size of the solid product were characterized on a JSM-6700F scanning electron microscopy (SEM) and a JEOL JEM2010 transmission electron microscope (TEM) at 200 KV. The content of Eu was determined by ICP-AES. Specific surface area of the sample was measured with an Accelerated Surface Area and Porosimetry analyzer (Micromeritics' ASAP 2020).

Results and Discussion

Synthesis and characterisation. The GO@TiP composite was synthesized by a facile solution-phase reaction. The synthesis process is illustrated in Figure 1. When added to GO solution, titanium ions from titanium sulphate may bind to the functional groups such as carboxyl and hydroxyl on the surface of GO. Then, with the phosphate ion added, the Ti^{4+} from GO-Ti would probably reacts with PO_4^{3-} forming a precipitate and resulting in a GTiP nanocomposite with the bridging of Ti^{4+}.

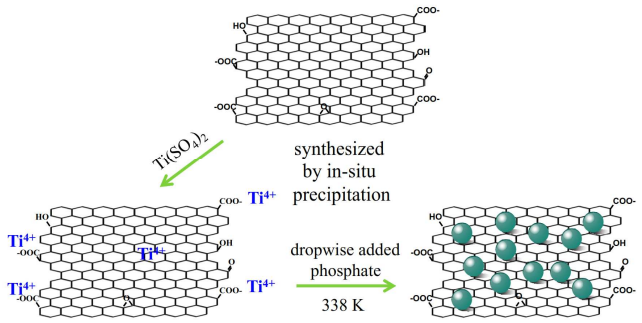

Figure 1. Schematic illustration of the formation of GTiP composites.

During the synthesis, different amounts of GO were added forming a series of products—TiP, GTiP-1, and GTiP-2. TiP was obtained without GO, while GTiP-1 and GTiP-2 were obtained at the C and Ti molar ratios of 1:1 and 4:1, respectively. The XRD patterns of GO, TiP, GTiP-1 and GTiP-2 are shown in Figure 2. The sharp (001) diffraction peak at 11.3° indicates the formation of GO.[20] The obtained GTiP-1 and GTiP-2 composites display a similar XRD pattern to TiP, implying that GO does not influence the phase structure of TiP. It should be noted that no diffraction peaks of GO can be found in the spectra of GTiP-1 and GTiP-2 samples. The reason might be due to the low content of GO as well as less stacking of GO layers in the (001) direction hindered by the composited TiP.

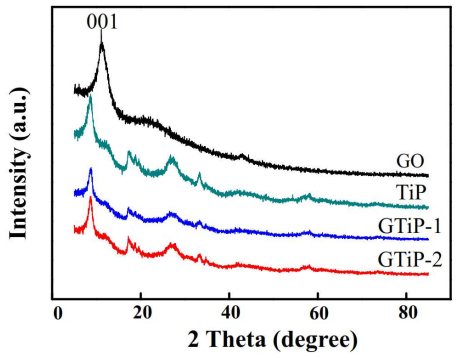

Figure 2. XRD spectra of GO, TiP, GTiP-1, and GTiP-2.

The XRD spectra of nanocrystallized TiP materials do not match any reference from ICSD. Thus, XPS analysis was conducted to deduce the surface state and composition of TiP. Atomic percentage content of TiP is shown in Table 1. The atomic percentages of O, Ti, and P are 57.34, 8.02 and 15.50, which approximate to a O:Ti:P ratio of 7:1:2. The wide-scan XPS spectra of TiP are shown in Figure S1. The photoelectron lines at binding energies of 132.85, 284.57, 459.25 and 531.03 eV, can be attributed to P 2p，C 1s，Ti 2p and O 1s, respectively. In the Ti 2P spectra (Figure S1 upper right), the binding energy of Ti $2p_{3/2}$ orbital is 459.25 eV, implying that Ti exists in a tetravalent state.[21] In the P 2p spectra (Figure S1 upper left), the peak 132.85 eV can be attributed to P 2p corresponding to pyrophosphate ($P_2O_7^{4-}$), which is in good agreement with element atomic ratio in Table 1.

Table 1 Element contents of TiP

Elements	C	O	Ti	P	Total
At. %	19.14	57.34	8.02	15.50	100

The macrographs of the materials are shown in Figure 3a, d, and g. It can be seen that the pure TiP is white, and as the added amount of GO increases, the colour of the samples gradually deepens to black. Figure 3b, e, h, c, f, and i are the SEM images of the above materials. Pure TiP forms full flowerlike pellets which are independent of each other and have a uniform size of about 1 μm. GTiP-1 has nearly the same morphology as TiP with some GO sheets evenly distributed under the flower-like pellets. When the composites contain more GO, TiP transforms into a cascade-crisscross structure.

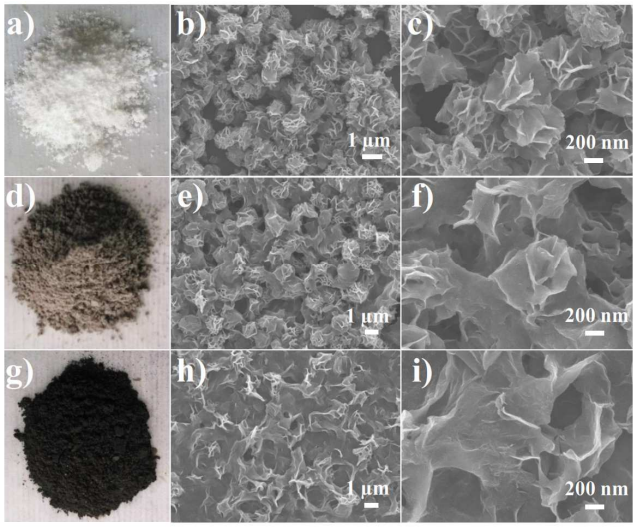

Figure 3. a, d, and g are the macrographs and b, c, e, f, h, and i are the SEM images of TiP, GTiP-1, GTiP-2, respectively.

The TEM images (Figure 4) of GTiP-1 and GTiP-2 further confirm the SEM results. TiP and GO are composited together well in both nanomaterials. GTiP-1 mainly exists as flowerlike pellets and GTiP-2 exists as wrinkling sheets. Figure 4c is a partial TEM image of GTiP-1. The lighter (A) and darker (B) areas can be attributed to TiP, and GO, respectively. Further elements mapping (Figure 4d-g) indicates that area A contains carbon (from GO), and area B contains O, P, and Ti element (from TiP). It implies that GO and TiP are not simply mixed, but grow together symmetrically.

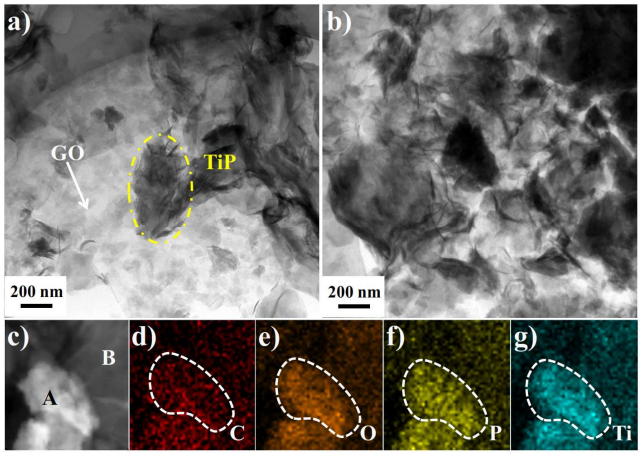

Figure 4. a and b are the TEM images of GTiP-1 and GTiP-2, respectively. c is partial TEM images of GTiP-1. d, e, f, and g are the elements mapping of C, O, P, and Ti, respectively.

Figure S2 shows the N_2 adsorption-desorption isotherms of TiP, GTiP-1, and GTiP-2 at 77 K. With a clear hysteresis loop, the type IV isotherm curves indicate that all the three materials possess typical mesoporous structures.[22] The specific surface area of TiP, GTiP-1, GTiP-2 and GO are calculated to be 10.46, 43.38, 102.31 and 115.41 $m^2\ g^{-1}$, respectively, using a multi-point Brunauer-

Emmett-Teller (BET) method. With a greater content of GO, GTiP-2 possesses higher specific surface area than TiP and GTiP-1. It should be noticed that the BET of GTiP-2 and GO is about the same level with the huge discrepancy of GO content. The increase of specific surface area of the nanocomposites may be due to the intercalation of TiP particules, acting as spacers between GO sheets and avoiding their aggregation.[23] The BET data is consistent with SEM results discussed before. It can be expected that GTiP-1 and GTiP-2 should have superior adsorption performances thanks to these structural features.

Adsorption kinetic analysis. To evaluate the adsorption rate and efficiency of GO, TiP, GTiP-1 and GTiP-2 towards Eu^{3+}, time-dependent adsorption curves were generated (Figure 5). All four materials show a similar trend of a rapid adsorption stage in the first 20 min followed by a gradual increase approaching the steady state. Since the removal of Eu^{3+} occurred in such a short time, the adsorption of Eu^{3+} should mainly be attributed to chemical adsorption or surface complexation. The strong interaction between Eu^{3+} and GTiP derives from the carboxyl and hydroxyl groups on GO as well as the phosphate groups on TiP. Among the four materials, the composite adsorbents process higher saturated adsorption volumes comparing to the single GO or TiP. With a little GO added, GTiP-1 (mass ratio GO:TiP is about 1:19) has already shown a 116.6% enhanced adsorption capacity (equation S1) to the simply mixed GO and TiP. The pseudo second order model[24] can be used to fit the experimental data and identify the rate-limiting step (Figure 5b). Kinetic parameters obtained by linear regression are summarized in Table 2.

The pseudo second order kinetic model is expressed as:

$$\frac{t}{Q_t} = \frac{1}{kQ_e^2} + \frac{t}{Q_e} \quad (1)$$

where Q_e (mg g^{-1}) is the amount of Eu^{3+} adsorbed at equilibrium and Q_t (mg g^{-1}) is the amount of Eu^{3+} adsorbed at contact time t (min). k (g mg^{-1} min^{-1}) is the rate constant of the second-order adsorption. The values of Q_e and k are calculated from the intercept and slope of the plot of t/Q_t vs. t, respectively. The calculated Q_e of the four materials are very close to Q_t of 2 h, and the least amount of Eu^{3+} was adsorbed by TiP (16.02 mg g^{-1}) whereas the most by GTiP-2 (52.63 mg g^{-1}). The correlation coefficients (R^2) for the pseudo-second-order model all exceed 0.99. The high correlation coefficient and the agreement between calculated and experimental Q_e values both suggest that the kinetic adsorption of Eu^{3+} on these materials follows the psedo-second-order model, implying that the rate-limiting step may be the chemical adsorption step.

In addition, the initial adsorption rate h (mg g^{-1} min^{-1}) and half-equilibrium time $t_{1/2}$ (min) are also listed in Table 2 as calculated using the following equations: [25,26]

$$h = kQ_e^2 \quad (2)$$

$$t_{1/2} = \frac{1}{kQ_e} \quad (3)$$

$t_{1/2}$, which is the time required for the adsorbent to reach a half-saturation state (when $t = t_{1/2}$, $Q_t = 0.5Q_e$), is often used as a measure of the adsorption rate. As shown in Table 2, $t_{1/2}$ values of TiP and the composites are all less than 1.5 min, hence TiP-containing materials can quickly remove Eu^{3+} from solutions. It should also be noted that the adsorption rate of GO is slower than the others with a $t_{1/2}$ value of 5.05 min.

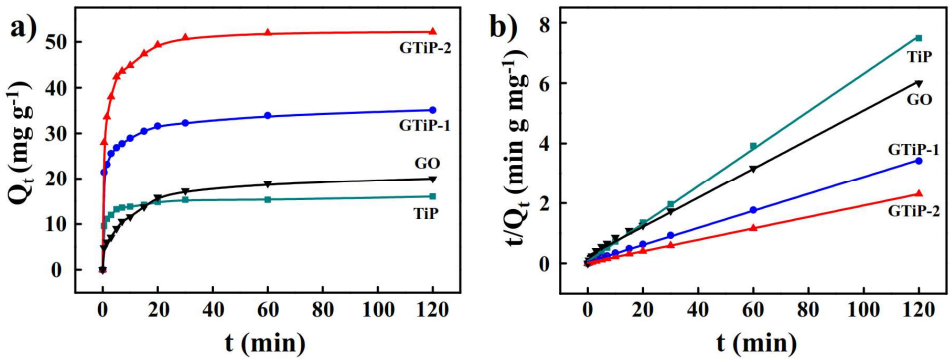

Figure 5. (a)Adsorption of Eu^{3+} on GO, TiP, GTiP-1 and GTiP-2 as a function of contact time. (b) t/Qt vs. t plots for the four types of materials. The initial concentration of Eu^{3+} is 100 mg L^{-1}, pH=5.5 and the dosage of adsorbent is 1mg mL^{-1}.

Table 2. Kinetic parameters for the adsorption of Eu^{3+} fitted by the pseudo-second-order kinetic model.

	Q_e (mg g^{-1})	k (g mg^{-1} min^{-1})	R^2	h (mg g^{-1} min^{-1})	$t_{1/2}$ (min)
TiP	16.02	0.054	0.9994	13.86	1.16
GO	20.62	0.0096	0.9955	4.08	5.05
GTiP-1	35.21	0.019	0.9993	23.55	1.49
GTiP-2	52.63	0.018	0.9998	49.86	1.05

Adsorption isotherm. To further access the adsorption capacity of GTiP-2, Eu^{3+} adsorption experiments by 1 g L^{-1} GTiP-2 at various initial Eu^{3+} concentrations ranging from 5 to 200 mg L^{-1} were performed. Experimental and fitted results are shown in Figure 6. Two common isotherm equations (Langmuir and Freundlich) were adopted to fit the experimental data by non-linear regression.

$$\text{Langmuir} \qquad Q_e = \frac{Q^0 b C_e}{1 + bC_e} \quad (4)$$

$$\text{Freundlich} \qquad Q_e = kC_e^{\frac{1}{n}} \quad (5)$$

where Q_e is the amount adsorbed at equilibrium (mg g^{-1}). C_e is the equilibrium concentration (mg L^{-1}). Q^0 is the maximum adsorption capacity (mg g^{-1}). b is a constant related to the binding strength (L mg^{-1}). n and k are constants indicative of adsorption strength and adsorption capacity, respectively.

The results show that the Langmuir and Freundlich models are both appropriate to depict the adsorption of Eu^{3+}. Since the value of

the Freundlich constant n equals 3.44 (Table 3), which lies between 1 and 10, the adsorption of Eu^{3+} onto GTiP-2 is favoured. It is apparent in Figure 6 that the Langmuir isotherm fits the experimental data better than the Freundlich isotherm. The adsorbed amount at saturation Q^0 (64.33 mg g^{-1}), as obtained by the Langmuir fitting, was much higher than most of adsorbents in the previous studies. It is a good adsorbent for Eu^{3+} in aqueous solutions.

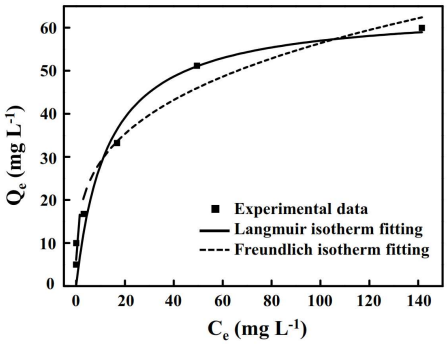

Figure 6. Adsorption isotherms of Eu^{3+} by GTiP-2 and fitting by Langmuir and Freundlich models. The dosage of GTiP-2 was 1 g L^{-1}, pH = 5.5, T =298 K.

Table 3. Langmuir and Freundlich constants associated with adsorption isotherms of Eu^{3+} on GTiP-2

Langmuir	Q^0 (mg g^{-1})	b (L mg^{-1})	R^2
	64.33	0.077	0.93
Freundlich	k	n	R^2
	14.81	3.44	0.97

Effects of pH and ionic strength. In real rare-earth industrial wastewater, factors such as pH and salinity are vital for the recycling performance.[27] Considering that most of Eu-containing wastewater samples are acidic or neutral, four pH values (1.7, 3.7, 5.5 and 7.3) were chosen in this work. The pH-dependent adsorption of Eu^{3+} on TiP, GO, GTiP-1 and GTiP-2 were studied and the results are shown in Figure 7a. Generally, the adsorption capacities of most adsorbents for metal ions increase with pH. In this work, TiP, GO and their nanocomposites behave similarly to most adsorbents. At pH 1.7, a large number of protons compete with Eu^{3+} for the $–COO^-$, $–O^-$ and $–P–O^-$ sites on the adsorbent, resulting in a lower adsorption capacity. As pH increases from 3.7 to 7.3, more and more $–COO^-$, $–O^-$ and $–P–O^-$ sites open up, allowing increased adsorption of Eu^{3+} by electrostatic interaction. Moreover, it was reported that Eu^{3+} would transform into $Eu(OH)^{2+}$, $Eu(OH)_2^+$ and $Eu(OH)_3$ at the pH above 6.5.[6] This may explain the sudden surge in adsorption capacity from pH 5.5 to 7.3. It can also be observed that GTiP-1 and GTiP-2 show considerably high adsorption capacities over a broad range of pH from 3.7 to 7.3, which is superior to GO or TiP. Even at pH as low as 3.7, the adsorption capacities of GTiP-1 and GTiP-2 are still quite high. This shows the effectiveness of these composite adsorbents in direct uptaking Eu^{3+} from acidic solutions.

Eu^{3+} uptake as a function of ionic strength controlled by various Na^+ concentrations is shown in Figure 7b. No significant change in the adsorption capacity can be observed for GTiP-1 and GTiP-2 in the ionic strength range from 1 to 1000 mM. It implies that complexation is the dominant mechanism for Eu^{3+} immobilization on GTiP nanocomposites. Specific coordinate covalent bonds were formed between Eu^{3+} and the electron-donating groups (i.e., $–COO^-$, $–O^-$ and $–P–O^-$ binding sites) on GTiP surfaces. Salinity is not an issue when this type of Eu^{3+} adsorbents is used in wastewater.

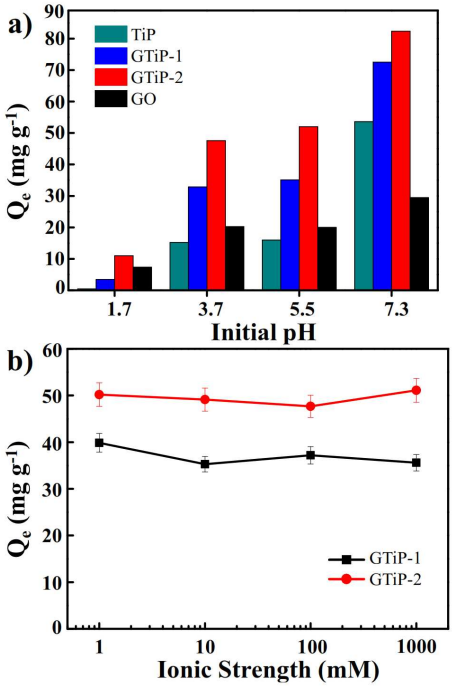

Figure 7. a) Adsorption capacities of GO, TiP, GTiP-1 and GTiP-2 for Eu^{3+} with different initial pHs. b) Adsorption capacities of GTiP-1 and GTiP-2 as a function of ionic strength at pH 5.5. Conditions: T = 298 K, C_{Eu} = 100 mg L^{-1}. The dosage of adsorbent was 1 mg mL^{-1}.

Preconcentration strategy. Recycling and reuse of the adsorbent is necessary for economic reasons. Since the composite adsorbents performed poorly at low pH, an acid treatment with 1 M HCl was selected for the regeneration of GTiP. The strategy of Eu^{3+} preconcentration by GTiP nanocomposite is shown in Scheme 1. Upon the addition of GTiP to the Eu^{3+}-containing wastewater, Eu^{3+} spontaneously binds to the functional groups on the surface of GTiP by chemical adsorption and/or complexation. At equilibrium, the adsorbent can be separated from the solution by filtration or centrifugation. Subsequently, the Eu^{3+}-adsorbed GTiP is washed in a small amount of 1 M HCl solution to desorb Eu^{3+}. The adsorbent can be reused after washing with DI water 3 times. The pre-enrichment step can be repeated in the same HCl solution for several times. The concentration of Eu^{3+} can be enriched a few dozen times. Eventually, the concentrated Eu^{3+} can be precipitated by oxalic acid and europium oxide can be obtained by calcination.

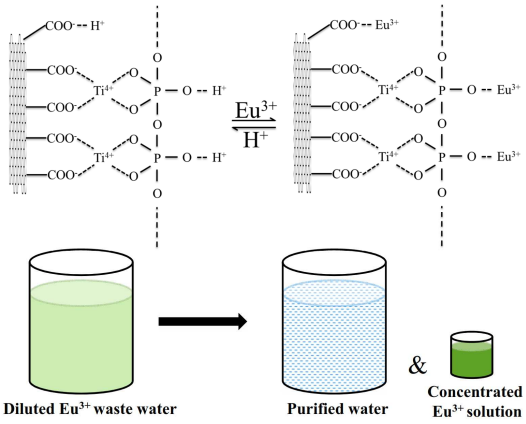

Scheme 1. Preconcentration strategy for Eu^{3+}-containing wastewater with GO-TiP nanocomposite.

Regeneration and recycle. The adsorption/desorption cycles were repeated four times using the same batch of GTiP-1 and GTiP-2 (Figure 8). Comparing to the first cycle, the adsorption capacity of GTiP-1, GTiP-2 at the forth cycle decreased from 35.08 to 24.91 mg g^{-1} and from 52.00 to 37.29 mg g^{-1}, respectively, revealing good regeneration and reusability. The concentration of Eu^{3+} is enriched from 100 mg L^{-1} to 1.75 g L^{-1}. The slight decrease in the adsorption capacity might be mainly owing to the incomplete desorption of Eu^{3+} from the surface of adsorbents and the increasing Eu^{3+} concentration of the eluant during recycling. For Eu^{3+} ions that penetrate into the vacant sites of GTiP, desorption may be more difficult. Figure S3 shows the SEM images of fresh and regenerated GTiP-1 after four cycles. Although the surface appeared rough and some broken spheres were observed, the regenerated composites still maintained the flowerlike structure. The C, Ti molar ratio of GTiP-1 rose from 1 to 1.27 with the BET changing from 43.38 to 77.65 m^2 g^{-1}, suggesting a small amount of titanium ions dissolved or detached from the composites during the process of adsorption/desorption cycles. The BET growth of the regeneration GTiP-1 may derive from the rising of carbon content, and the intercalation of TiP maintained the structure. Overall, the nanocomposites can be regenerated and reused several times, which supports their long term use in water treatment.

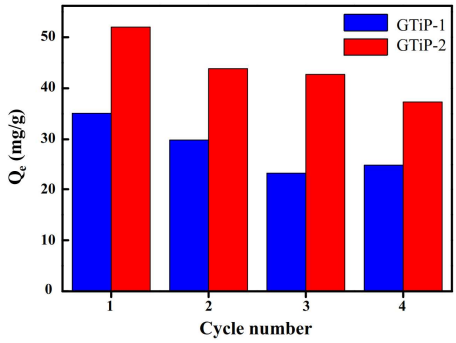

Figure 8. Regeneration studies of GTiP-1 and GTiP-2 in the uptake of Eu^{3+}. The dosages of the composites were 1 g L^{-1}, the initial concentration of Eu^{3+} was 100 mg L^{-1} and the contact time was 2 h.

Conclusions

In summary, GO@TiP nanocomposites were synthesised by an in-situ precipitate method. The as-prepared GTiP composites can be well dispersed in water, which solves the problem that dried GO can hardly dispersed for the strong forces between GO layers. Adsorption of Eu^{3+} on GTiP was systematically studied. The GTiP composites showed enhanced adsorption capacity for Eu^{3+} as compared to TiP or GO. Moreover, GTiP showed great adsorption ability both in a wide range of pH and salinity. Interestingly, the GTiP composites exhibited a self-supported structure, which can avoid aggregation and clogging problems with GO alone. This work would help design systems for recycling europium or other radioactive actinides from large volumes of wastewater.

Author Information

Corresponding Author:
*E-mail: zlin@fjirsm.ac.cn. Tel/Fax: (+086)591-83705474.

Acknowledgements

Financial support was provided by the National Basic Research Program of China (2010CB933501, 2013CB934302), the Outstanding Youth Fund (21125730), the National Science Foundation Grant (21273237, 21103191), the Knowledge Innovation Program of the Chinese Academy of Sciences (KJCX2-YW-N50, KJCX2EW-J02), and the Fujian Science Foundation Grant (2012J05035).

Notes and references

[a] State Key Laboratory of Structures, Fujian Institute of Research on the Structure of Matter, Chinese Academy of Sciences, Fuzhou, Fujian, 350002, China

1 A. Hosseini, J. E. Brown, J. P. Gwynn and M. Dowdall *The Science of the total environment* 2012, **438**, 325-333.
2 A. Adamantiades and I. Kessides *Energy Policy* 2009, **37**, 5149-5166.
3 C. Kelley, R. E. Mielke, D. Dimaquibo, A. J. Curtis and J. G. Dewitt *Environmental science & technology* 1999, **33**, 1439-1443.
4 Q. H. Fan, X. L. Tan, J. X. Li, X. K. Wang, W. S. Wu and G. Montavon *Environmental science & technology* 2009, **43**, 5776-5782.
5 C. E. Cui, H. Liu, P. Huang and L. Wang *Journal of Luminescence* 2014, **149**, 196-199.
6 X. Tan, M. Fang, J. Li, Y. Lu and X. Wang *Journal of hazardous materials* 2009, **168**, 458-465.
7 X. Tan, Q. Fan, X. Wang and B. Grambow *Environmental science & technology* 2009, **43**, 3115-3121.
8 S. Yang, P. Zong, X. Ren, Q. Wang and X. Wang *ACS applied materials & interfaces* 2012, **4**, 6891-6900.
9 Y. Sun, C. Chen, X. Tan, D. Shao, J. Li, G. Zhao, S. Yang, Q. Wang and X. Wang *Dalton transactions* 2012, **41**, 13388-13394.
10 C. L. Chen, X. K. Wang and M. Nagatsu *Environmental science & technology* 2009, **43**, 2362-2367.
11 Y. Sun, Q. Wang, C. Chen, X. Tan and X. Wang *Environmental science & technology* 2012, **46**, 6020-6027.
12 H. Wang, X. Yuan, Y. Wu, H. Huang, G. Zeng, Y. Liu, X. Wang, N. Lin and Y. Qi *Applied Surface Science* 2013, **279**, 432-440.
13 G. Zhao, J. Li, X. Ren, C. Chen and X. Wang *Environmental science & technology* 2011, **45**, 10454-10462.
14 R. Sitko, E. Turek, B. Zawisza, E. Malicka, E. Talik, J. Heimann, A. Gagor, B. Feist and R. Wrzalik *Dalton transactions* 2013, **42**, 5682-5689.
15 Y. Yuan, G. Zhang, Y. Li, G. Zhang, F. Zhang and X. Fan *Polymer Chemistry* 2013, **4**, 2164.
16 Y. L. F. Musico, C. M. Santos, M. L. P. Dalida and D. F. Rodrigues *Journal of Materials Chemistry A* 2013, **1**, 3789.
17 C. Li, Z. Zhuang, F. Huang, Z. Wu, Y. Hong and Z. Lin *ACS applied materials & interfaces* 2013, **5**, 9719-9725.
18 B. B. Sahu and K. Parida *Journal of colloid and interface science* 2002, **248**, 221-230.
19 W. S. Hummers and R. E. Offeman *Journal of the American Chemical Society* 1958, **80**, 1339-1339.
20 F. J. Chen, Y. L. Cao and D. Z. Jia *CrystEngComm* 2013, **15**, 4747.
21 J. F. Moulder, W. F. Stickle, P. E. Sobol and K. D. Bomben 1992.
22 B. J. Li, H. Q. Cao and G. Yin *Journal of Materials Chemistry* 2011, **21**, 13765-13768.
23 P. Montes-Navajas, N. G. Asenjo, R. Santamaria, R. Menendez, A. Corma and H. Garcia *Langmuir* 2013, **29**, 13443-13448.
24 Y. S. Ho and G. Mckay *Process Safety and Environmental Protection* 1998, **76**, 332-340.

25 Demirbaş, Y. Turhan and M. Alkan *Desalination and Water Treatment* 2014, 1-8.

26 Q. Cao, F. Huang, Z. Zhuang and Z. Lin *Nanoscale* 2012, **4**, 2423.

27 X. L. Tan, Q. H. Fan, X. K. Wang and B. Grambow *Environmental science & technology* 2009, **43**, 3115-3121.

Table of Contents Entry

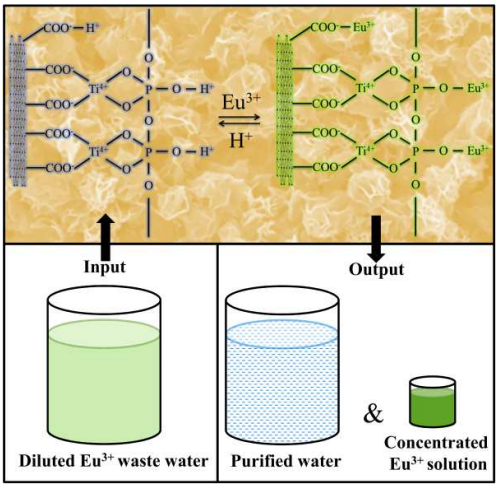

Titanium Phosphate@Graphene Oxide nanocomposites exhibit enhanced hydrophilicity, adsorption capacity and efficiency on Eu3+ enrichment.